Hindawi
Journal of Sensors
Volume 2019, Article ID 6941907, 11 pages
https://doi.org/10.1155/2019/6941907

Research Article

Adaptive Triangular Deployment of Underwater Wireless Acoustic Sensor Network considering the Underwater Environment

Woojoong Kim,[1] **Hyun Wook Moon**,[2] **and Young Joong Yoon**[1]

[1]*Department of Electric and Electronic Engineering, Yonsei University, Seoul 120-749, Republic of Korea*
[2]*ISR R&D Lab, LIG Nex1, Yongin City, Gyeonggi-do 148-1, Republic of Korea*

Correspondence should be addressed to Young Joong Yoon; yjyoon@yonsei.ac.kr

Received 6 June 2018; Revised 20 October 2018; Accepted 28 October 2018; Published 25 February 2019

Academic Editor: Christos Riziotis

In this paper, we propose an adaptive triangular deployment algorithm that can adjust sensor distribution depending on the variation in communication performance in an underwater environment. To predict the distance between sensor nodes, a performance surface model is implemented by estimating the communication performance based on spatio-temporal environment factors affecting the communication performance of the underwater sensor node. Subsequently, the performance surface model is applied to the adaptive triangular deployment algorithm and is used to control the distance between nodes. Therefore, underwater wireless sensor networks deployed with adaptive triangular deployment algorithms can achieve a maximum connectivity rate with an optimal number of nodes.

1. Introduction

The nodes constituting a wireless sensor network collect various information from the environment and transmit this data to the adjacent nodes [1]. The layout of a sensor network is important for the efficient and stable functioning of the nodes. Therefore, research on a deployment algorithm for determining the optimal layout of a sensor network by adjusting the position of nodes in a given area is extremely important in sensor networks.

Deployment algorithms can be divided into two categories: random deployment algorithms and deterministic deployment algorithms [2]. Random deployment algorithms are suitable when the nodes are arranged without any limitation with regard to the number of sensor nodes. After random deployment is performed, we can ensure stability by deploying additional nodes in the area where degraded performance of the system is observed. In the case of deterministic deployment, an algorithm deploys the nodes in a predetermined position by considering the performance of the current sensor nodes. The deployment of the terrestrial sensor network is suitable for applying the random deployment algorithm because the cost of the node is low and the performance change of the sensor node is not large depending on the position within a given area. On the contrary, in an underwater environment, the performance of the sensor node is highly variable even within a given area. When the sensor nodes are randomly deployed in a region where the performance of nodes is not homogeneous, the connectivity between the nodes degrades due to deterioration in communication performance in some areas. In another area, more nodes than necessary can be deployed even though sufficient connectivity is secured. Although the performance of the network can be improved by deploying additional nodes in the area where the number of nodes is insufficient even though there are redundant nodes in some areas, this hinders the economics of network implementation. In particular, this method is not suitable owing to the high cost of an underwater sensor node.

Numerous deterministic deployment algorithms have been studied, and some of them are summarized in Table 1. Particle swarm optimization (PSO) and virtual force algorithm (VFA) are deployment algorithms based on optimization algorithms and are used to find the optimal sensor node position through iterations until the initial random deployment node satisfies the given condition [3, 4]. Optimization

Table 1: Example of a sensor deployment algorithm.

Reference	Algorithm	Criterion	Adjust sensor spacing
[3]	Optimization	Coverage	Impossible
[4]	Optimization	Coverage	Impossible
[5]	Pattern	Coverage	Impossible
[6]	Pattern	Coverage	Impossible
[7]	Pattern	Coverage	Impossible
[8]	Pattern	Coverage, partial connectivity	Impossible
[9]	Pattern	Coverage, partial connectivity	Impossible
This paper	Pattern	Full connectivity	possible

algorithms have the disadvantage that the time required to deploy a node increases exponentially as the number of nodes increases and the complexity of the environment increases. Another deterministic deployment technique is to deploy nodes in various patterns, such as triangles, long belts, and diamonds [5–9]. However, conventional pattern deployment algorithms mainly considered only the coverage between nodes [5–7]. In such a case, as there is a possibility that each node of the sensor networks cannot transmit the collected data to the adjacent nodes, the function of the sensor networks may be lost. Although some studies have proposed a deployment considering connectivity, their results pertain to limited conditions and only considered partial connectivity [8, 9]. In case of partial connectivity, managing the information delivery time and lifetime of nodes is disadvantageous because it is more likely to bypass more nodes to transmit the collected information to the final node. In addition, when one node fails, there is a possibility that the connectivity of the entire node becomes problematic. As it is not easy to find and replace the problematic nodes after the underwater sensor network is configured, it is necessary to deploy the nodes to enable communication between the nodes through an alternative path. Crucially, conventional pattern deployment algorithms are unsuitable for underwater environments where the performance of the sensor varies rapidly depending on the environment, as all nodes assume the same detection or communication range.

In this paper, an adaptive triangular deployment algorithm is proposed to obtain maximum connectivity with the optimal number of nodes based on the simulated communication performance of sensor nodes in an underwater environment. Most conventional triangular deployment algorithms deploy nodes at equal distances, which can theoretically form full connectivity with adjacent nodes [9]. However, as the performance of the nodes may vary depending on the environment they are in, if equally spaced deployment is applied, connectivity between nodes in all areas can be difficult to maintain, and there may be some areas where the nodes may not be connected. In our proposed adaptive triangular deployment algorithm, node deployment is possible by adjusting the node interval by considering the communication performance depending on the node positions in a given area. Therefore, it is more advantageous than the conventional triangular deployment algorithm in ensuring connectivity between nodes. The communication performance in a given area is analysed through a communication prediction simulation that reflects the environmental factor affecting the node's communication performance, and a performance surface model is implemented by mapping the communication performance. The implemented performance surface model is used as the basis for adjusting the spacing of the adaptive triangular deployment algorithm, ensuring full connectivity of deployed nodes. Therefore, it is possible to construct an underwater sensor network that maintains high connectivity with an optimal number of nodes using an adaptive triangular deployment algorithm considering communication performance in an underwater environment.

This remainder of this paper is organized as follows. The generation method of the performance surface is described in Section 2. The methodology of the adaptive triangular deployment algorithm is proposed in Section 3. The adaptive triangular deployment algorithm is verified to be an efficient deployment method compared to the conventional triangular deployment algorithm via simulation comparisons in Section 4. The conclusions are summarized in Section 5.

2. Performance Surface Model

In conventional research, a performance surface model is used to geospatially map the detection probabilities of targets for the performance evaluation of underwater sonar systems [10]. In this paper, the communication range between nodes according to the underwater environment in a given area is calculated through simulation. An underwater communication performance surface model is implemented based on the communication range calculated for the whole given area. The performance surface model is used as a basis for position control considering the connectivity between nodes with the adaptive triangular deployment algorithm. This section describes the implementation process of the performance surface in detail.

2.1. Communication Distance Calculation with the Predicted Communication Performance. The communication performance of the sensor node can be evaluated through the bit error rate (BER) [11]. Therefore, the connectivity of two nodes is secured when two adjacent nodes constituting the sensor network satisfy the BER criterion required by the system. To estimate the BER between adjacent nodes in an

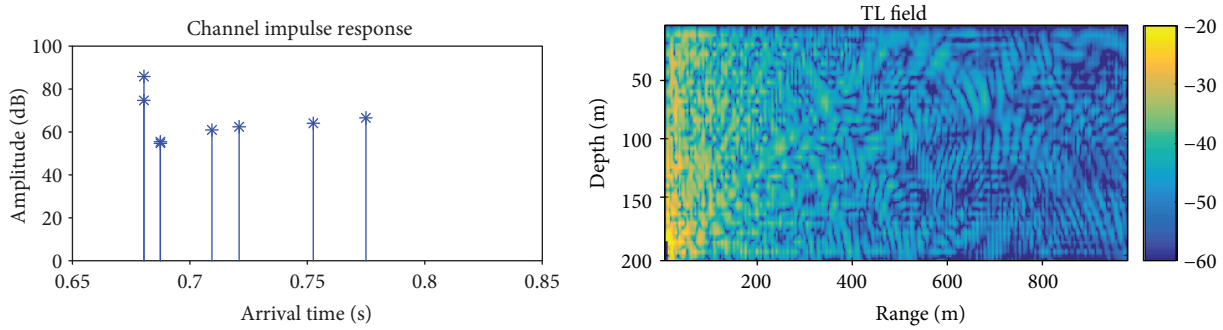

(a) Channel impulse response (b) Transmission loss

Figure 1: Simulated channel impulse response and transmission loss as obtained by the Bellhop model.

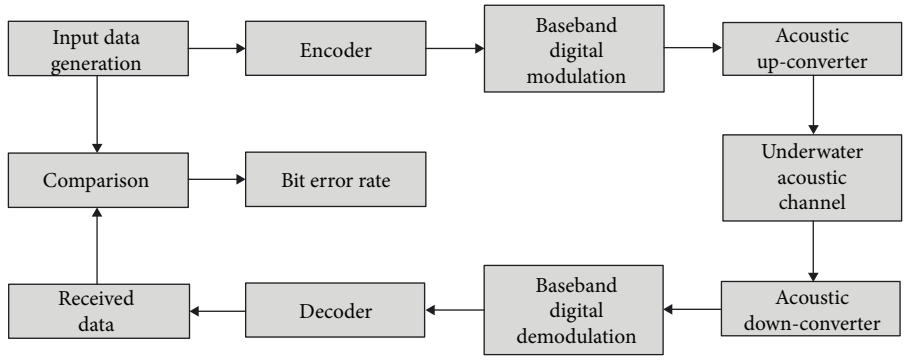

Figure 2: Block diagram of the communication performance estimation algorithm.

underwater environment, simulating the channel that reflects environmental information such as sound velocity profile, bathymetry, and bottom constituent depending on the location of the node is necessary. The Bellhop model is a suitable channel model to simulate an underwater acoustic channel reflecting environmental information, and it can extract channel impulse response and transmission loss, as shown in Figure 1 [12].

The signal-to-noise ratio (SNR) of the signal received at the receiving node can be calculated by including the simulated transmission loss (TL) value in Equation (1)

$$\mathrm{SNR} = \mathrm{SL} - \mathrm{TL} - \mathrm{NL}, \tag{1}$$

where SL denotes the source level and NL denotes the ambient noise level from the Wenz curve [13–15].

It is possible to represent an acoustic channel in the given underwater environment using the simulated channel impulse response characteristic and the calculated SNR value. The simulated channel impulse response and the calculated SNR are applied to the communication performance estimation algorithm, as shown Figure 2.

Figure 3 shows a deployment scenario of an underwater acoustic sensor network installed at the seabed. To obtain the communication range of each sensor node in the underwater environment, the maximum communication range (MCR) that satisfies the minimum BER for ensuring the stability of information transmission between adjacent nodes

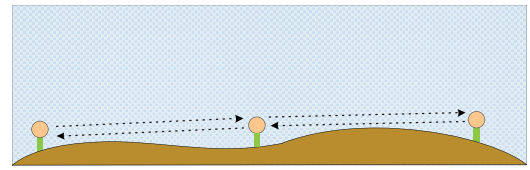

Figure 3: Deployment scenario of an underwater acoustic sensor network.

should be calculated. Therefore, the MCR can be calculated by extracting the BER depending on the distance from the transmitting node to the receiving node through the communication performance estimation algorithm.

2.2. Implementation of the Performance Surface Model in the Target Area. The East Sea of South Korea is selected as the target area for deploying the nodes. Figure 4 shows the sampling points for implementing the communication performance surface model in the target area. The selected target area spans an area of 16 km × 16 km, and there are a total of 25 sampling points in this area. Assuming that each sampling point denotes the location of the transmitting node, sampling was performed on the azimuth and the distance assuming that the receiving node exists for up to 2 km at intervals of 100 m for 6 azimuths. According to the deployment scenario in Figure 3, the sensor network is installed on the ocean floor; thus, the depth of the node is determined

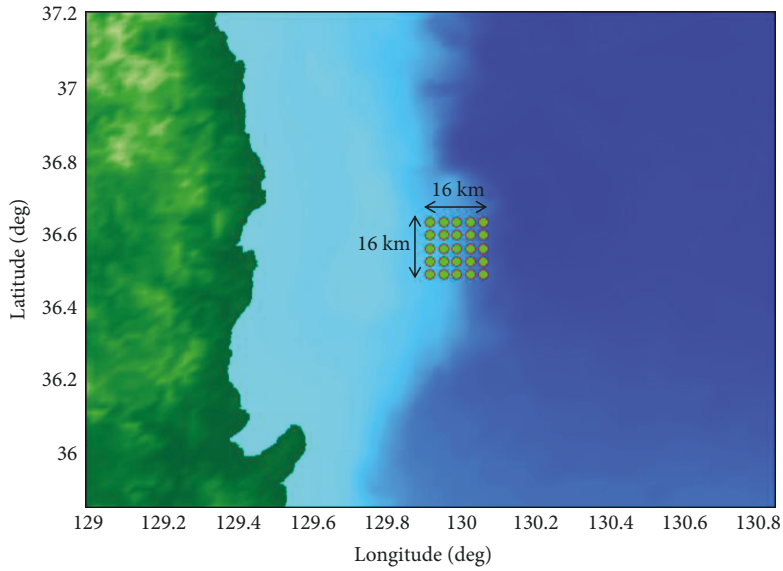

Figure 4: Sampling points in the target area.

by the topography of the position where the node is located. Therefore, the performance surface model is implemented assuming the horizontal distance based on the reference node. To simulate the communication channel for each sampling situation using the Bellhop model, the environmental data for sound velocity structure, topography, and bottom constituent were used. For the sound velocity structure, the monthly data of GDEM was used, and ETOPO data for bathymetry was used [16, 17]. The bottom constituent used data measured at the target area.

Topography and bottom constituent are spatial factors affecting the underwater communication channel, which vary with the location of the target area. The factor affecting the temporal change of the underwater channel is the sound velocity structure, which is sensitively affected by the temperature variation across seasons. The nodes constituting a sensor network must be able to communicate with the adjacent nodes in harsh environments. The sound velocity profile for various seasons should be considered for temporal change as well as spatial change. Therefore, a performance surface model with the sound velocity structure in February and August, which represents winter and summer, respectively, was implemented. Moreover, a comprehensive performance surface model is implemented by considering the lower performance value at each point of the two seasons.

Spatial SNR and BER for each azimuth and distance of the sampling points were simulated depending on the temporal and spatial changes of the underwater environment. The input parameters for the simulation are presented in Table 2, and the results for winter and summer are presented in Figures 5 and 6, respectively. Assuming a target BER of 1% as shown in Table 1, the MCR for each azimuth for each sampling point is calculated. As each sampling point has the MCR for each azimuth, each sampling point should be represented by its MCR in order to be simplified as a performance surface model. Therefore, the MCR is averaged over

Table 2: Communication system parameters for simulation.

Input Parameter	Value
Frequency	10 kHz
Source level	140 dB
Source depth	2 m above seabed
Receiver depth	2 m above seabed
Wind speed	5 m/s
Channel estimator	MMSE
Equalizer	MMSE
Target BER	1%

all azimuths at each sampling point using Equation (2), and this value is defined as the average maximum communication range (AMCR).

$$\text{AMCR} = \frac{\sum_{n=1}^{m} \text{Maximum communication range}}{\text{Number of bearing}}, \quad (2)$$

where m is the number of bearing samples.

Figures 7(a) and 7(b) show the performance surface model results of sensor nodes in winter (February) and summer (August), respectively. In summer, there are many refracted waves owing to the sound velocity structure, which causes communication performance degradation owing to the multipath delay spread of the signal. Therefore, the communication performance is relatively poorer in summer than in winter. Figure 8 shows the final performance surface model implemented by combining the performance surface models of the two seasons in the target area, which almost follows the performance surface model in summer.

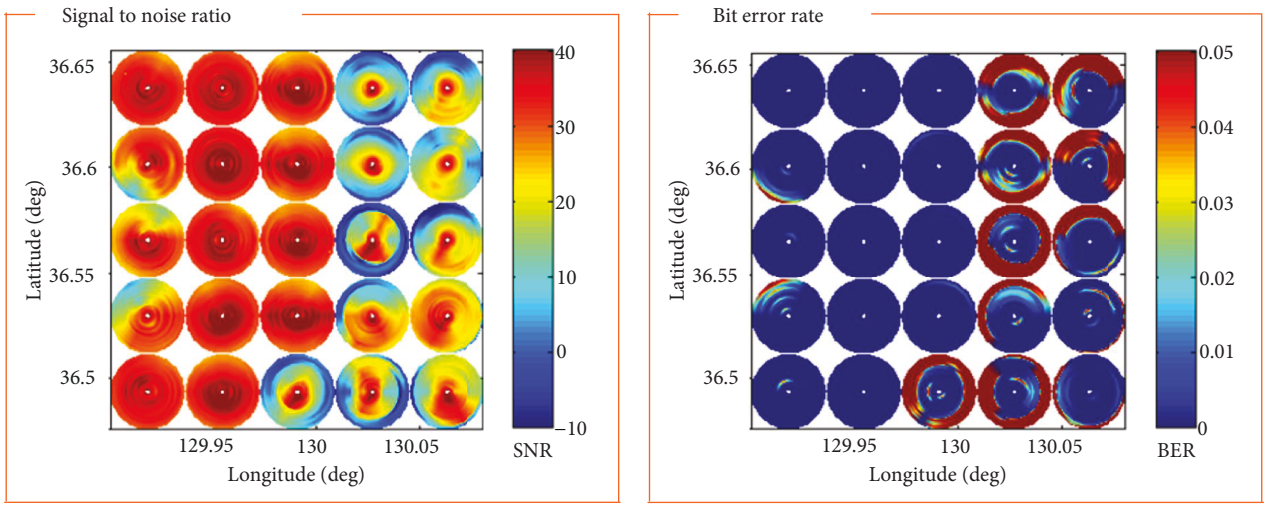

(a) SNR (b) BER

Figure 5: Signal to noise ratio (SNR) and bit error rate (BER) in winter (February) for the target area.

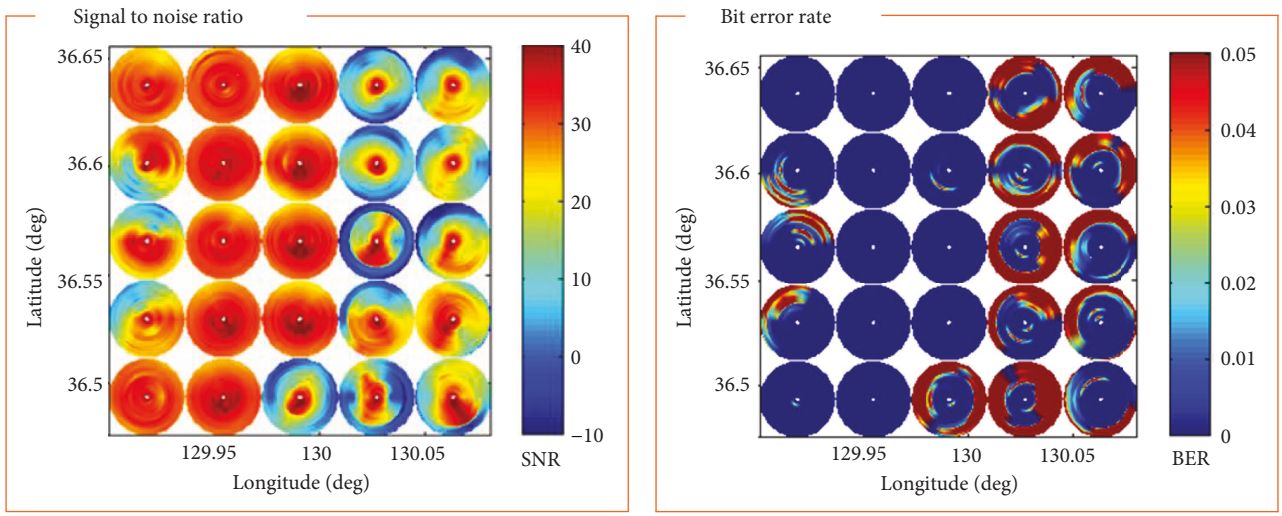

(a) SNR (b) BER

Figure 6: SNR and BER in summer (August) for the target area.

3. Methodology of Adaptive Triangular Deployment Algorithm

In the conventional triangular deployment algorithm, the distance between sensor nodes is constant [9]; it is impossible to adjust these distances based on the communication performance according to the positions of the nodes. Therefore, to effectively deploy sensor nodes in the underwater environment, an unequal spacing deployment algorithm that considers the changes in communication performance is required. In this study, the adaptive triangular deployment algorithm, which is capable of adjusting the distances between the sensor nodes according to changes in communication performance, is proposed. The proposed adaptive triangular deployment algorithm is a deterministic algorithm that is suitable for implementing efficient underwater sensor networks and offers full connectivity.

The conceptual depictions of the conventional and adaptive triangular deployment algorithms are presented in Figures 9(a) and 9(b), respectively. As shown in Figure 9(a), the constant communication ranges of the nodes do not overlap when the communication performance of the nodes differ according to the environment because the conventional method deploys nodes at constant spacing. Therefore, the connectivity between the nodes is not maintained consistently. In the adaptive method, because the communication performance of the nodes according to the environment is considered as shown in Figure 9(b), communication ranges of the nodes can overlap via positional adjustments. The performance surface model used to adjust the node spacing

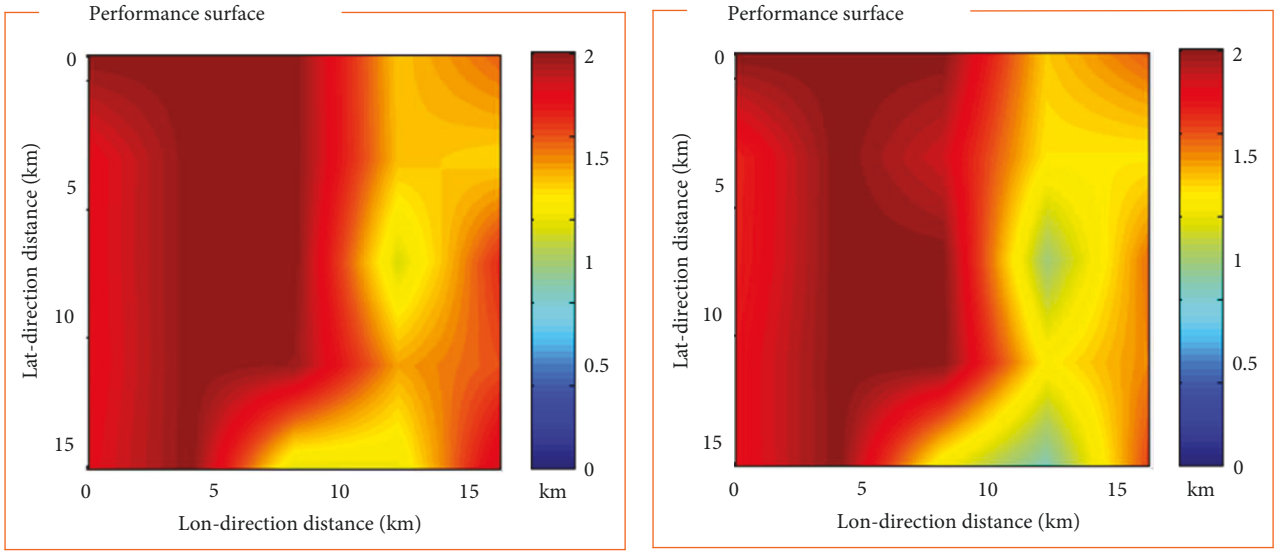

(a) Winter (b) Summer

Figure 7: Performance surface results of sensor nodes in winter (February) and summer (August).

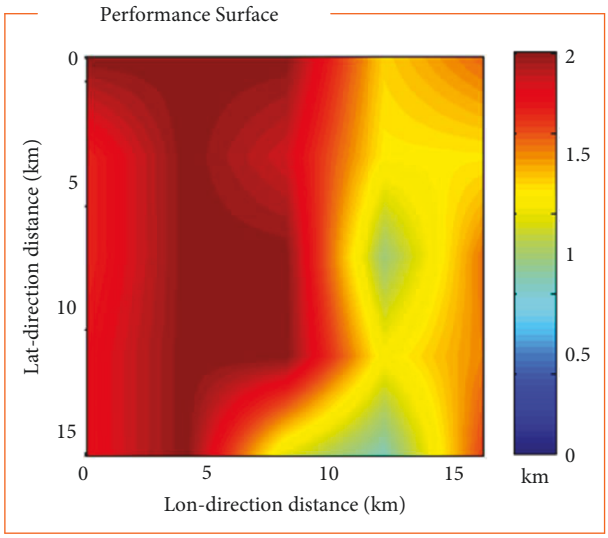

Figure 8: Final performance surface model implemented by combining the performance surface models of the two seasons in the target area.

in the proposed adaptive triangular deployment algorithm is represented by the AMCR that is azimuthally averaged at each sampling point; thus, the communication ranges of two adjacent nodes may be different. In general, the reciprocity theory is assumed between the transmitter and the receiver in a communication system. Applying the reciprocity theory to Figure 9(b), the communication ranges of nodes "b" and "c," which are located within the communication range of node "a," include the position of node "a." Therefore, we applied the reciprocity theory in the adaptive triangular deployment assuming that the connectivity of the two nodes is secured if the AMCR of one of these contains the remaining node's position.

Figure 10 shows the methodology of the adaptive triangular deployment algorithm. In this algorithm, the upper boundary of a target area is selected as the reference line, and the nodes in this line are deployed one by one horizontally. Node "A" is deployed as the reference node for the target area. Node "B" is deployed in the communication range of node "A" along the reference line. The communication range of node "A" can be extracted from the performance surface model of the target area, and the connectivity between nodes "A" and "B" can be secured by this method. The remaining nodes on the reference line are also deployed through this process to fill the line.

The nodes on the following line are deployed at the intersections between the communication ranges of the nodes on the preceding line. Node "a" is deployed at the intersection between the communication range of nodes "A" and "B." The intersection of the two nodes can be computed in vector form using Equation (3), and the progress is described in Figure 11.

$$\overrightarrow{OB} = \overrightarrow{OA} + \frac{\overrightarrow{AB}}{\overline{AB}} r_a \cos\theta + \left(\frac{\overrightarrow{AB}}{\overline{AB}}\right)^{\perp} r_a \sin\theta. \quad (3)$$

Node "b" is deployed at the intersection between the communication ranges of nodes "B" and "C." The nodes on this line are thus deployed using the same process to fill the entire line. This method is consecutively applied to all the even lines (see Figure 10).

If the aforementioned method is repeatedly applied to all the following lines, the number of nodes constituting each subsequent line decreases by one as shown in Figure 12; thus, it is impossible to deploy nodes for the entire target area by this method. To solve this problem, node "1" in Figure 10 is located on the intersection between the communication range of the node "a" and the left vertical boundary of the

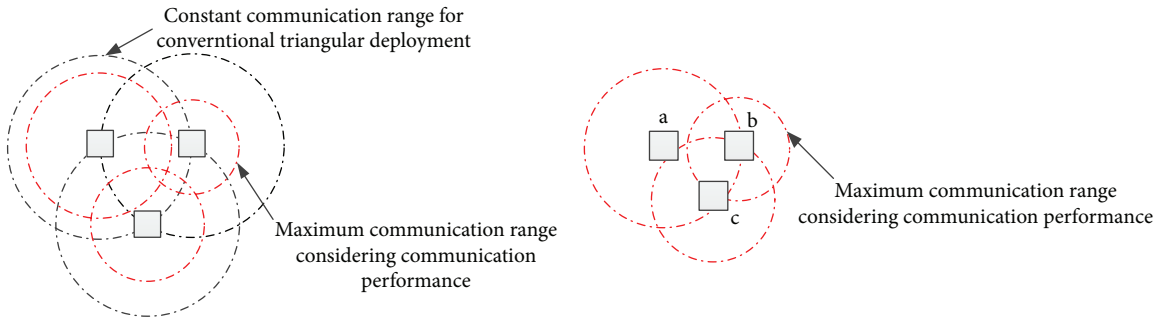

(a) Conventional triangular deployment algorithm (b) Adaptive triangular deployment algorithm

Figure 9: Conceptual depiction of the conventional triangular deployment algorithm (a) and adaptive triangular deployment algorithm (b).

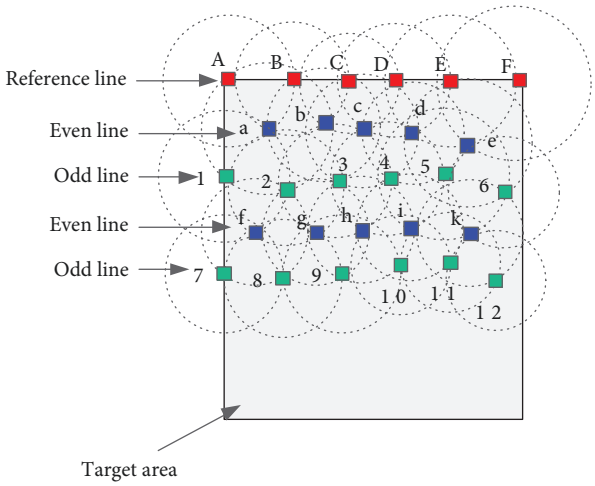

Figure 10: Methodology of the adaptive triangular deployment algorithm.

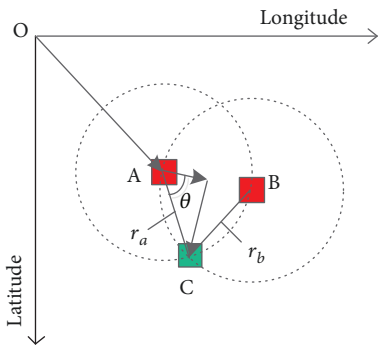

Figure 11: Method for finding the intersection between two nodes.

target area, serving as the new reference node. To ensure connectivity between node "1" and the nearest node of the upper line, node "2" is deployed at the intersection of the communication ranges of nodes "1" and "a," as shown in Figure 10. Further, node "3" is deployed on the intersection between the communication ranges of nodes "2" and "b." The nodes on this line are thus deployed in this manner to fill the entire line. The same method is consecutively applied to all the odd lines (see Figure 10).

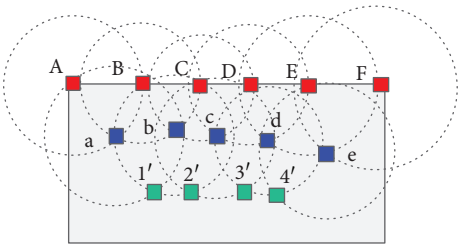

Figure 12: Adaptive triangular deployment using only the even line method.

Because a target area exhibits varied communication performance depending on the environment, it is sometimes impossible to determine an intersection using this proposed basic deployment method. Therefore, the following three techniques have been added to solve these problems.

First, if the condition of Equation (4) is not satisfied, no intersection exists between two nodes.

$$\sqrt{(x_a - x_b)^2 + (y_a - y_b)^2} \leq R_a + R_b, \tag{4}$$

where (x_a, y_a) and (x_b, y_b) are the coordinates of nodes "a" and "b," respectively. R_a and R_b are the communication ranges of nodes "a" and "b," respectively. For example, in Figure 13, node "3" is deployed at the intersection between the communication ranges of nodes "2" and "b" according to the odd line deployment method. However, because the distance between nodes "2" and "b" is greater than the sum of the communication ranges of the two nodes, Equation (4) is not satisfied, and there is no intersection between the two nodes. In this case, node "a," which was deployed before node "b," is used to determine the intersection for node "3." Thus, node "3" is deployed at the intersection between the communication ranges of nodes "a" and "2."

Second, when the deployment based on the performance surface model is implemented, a vertical position difference may occur between nodes on the same line. If this difference is accumulative, the intersection points between the nodes may not be readily obtained. Thus, a method to solve this problem is outlined in Figure 14. Nodes "A" and "B" on the same line have a slope $\propto$. If this slope exceeds the threshold,

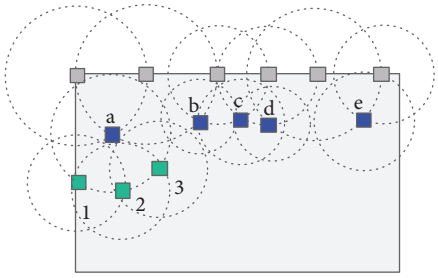

Figure 13: Deployment method when the distance between two nodes is greater than the sum of the communication ranges of the two nodes.

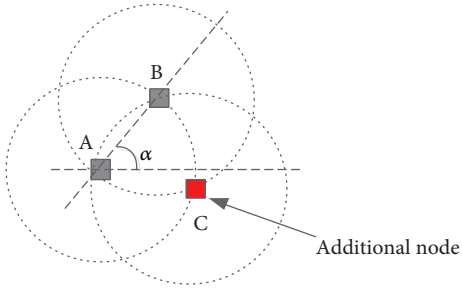

Figure 14: Principle of deployment of additional node using the tilt angle.

an additional node "C" is deployed at the intersection between the nodes "A" and "B."

Third, if there is a region where the communication performance is drastically degraded, a large number of nodes may be required to fill the given area, or the nodes may converge at a certain point without filling the given area. Therefore, selective deployment is required for an area that has rapidly declining performance. Accordingly, a limitation on the minimum communication range for deployment of a node should be defined. For example, if any node has a communication range below this limitation value, it is not deployed.

The flowchart of the adaptive triangular deployment algorithm is thus presented in Figure 15.

4. Simulation of Optimal Deployment of Sensor Nodes Using Adaptive Triangular Deployment Algorithm

The deployment of nodes using the aforementioned adaptive triangular deployment algorithm was performed by applying the performance surface model. To verify that the adaptive triangular deployment algorithm is effective for implementation and operation of an efficient and stable underwater sensor networks, it is compared with the conventional triangular deployment algorithm.

In the case of the conventional triangular deployment algorithm, because equal spacing is used with a constant communication range, a distance setting for the communication range is required. The communication range of 1 km (case 1) and 2 km (case 2) was selected via the best- and

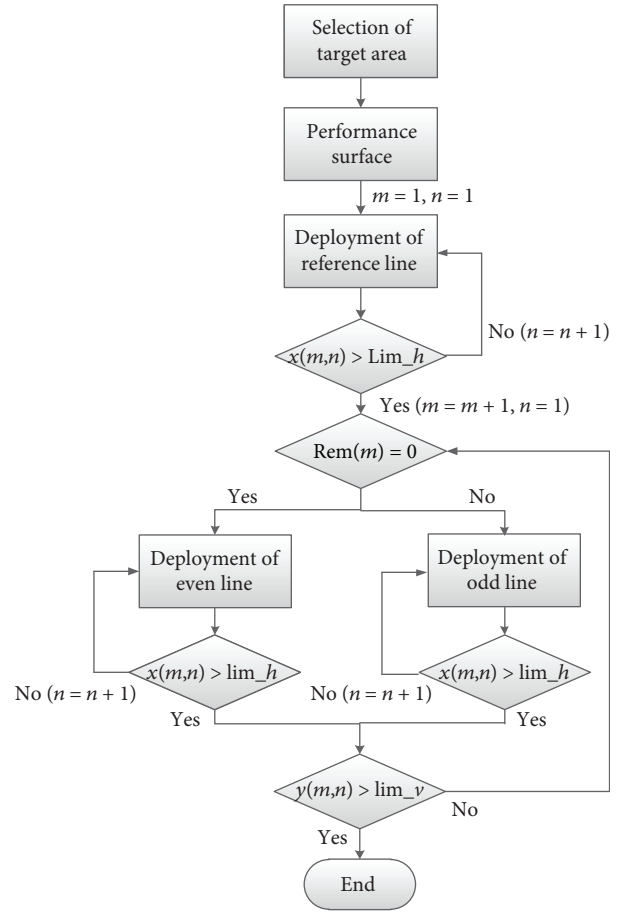

Figure 15: Flowchart of adaptive triangular deployment algorithm.

worst-case scenarios of the conventional triangular deployment algorithm, considering that the communication range in the given area from the performance surface model is approximately 1 km to 2 km. And 1.5 km (case 3) corresponding to the middle of both cases was selected as the communication range. The deployment results for each of these cases are shown in Figures 16–18. The deployment results are shown for the performance surface model and are located at constant spacing regardless of the communication ranges of the nodes according to their positions. Figure 19 shows the result of deploying nodes via the adaptive triangular deployment algorithm (case 4). The result is that the node distance is adjusted to reflect the communication range according to the position in the target area through the adaptive triangular deployment algorithm.

In Figure 20, the connectivity of sensor nodes for each case is illustrated. In case 1, connectivity between nodes was achieved in the entire given area, but more nodes are deployed in the area with superior communication performance. In cases 2 and 3, nodes in areas with low

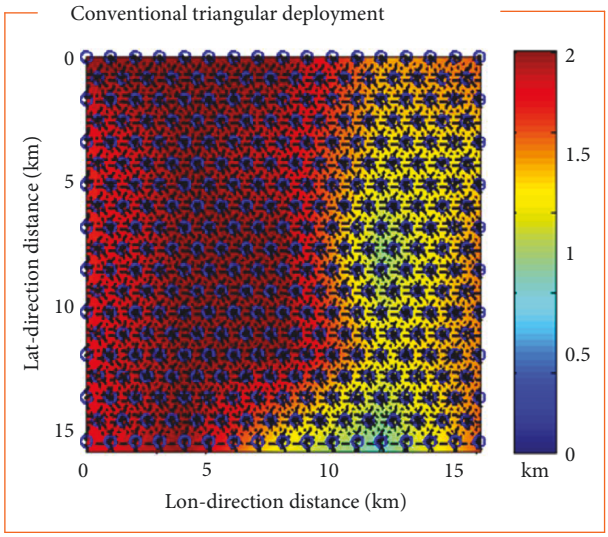

Figure 16: Deployment result using conventional triangular deployment within a range of 1 km (case 1).

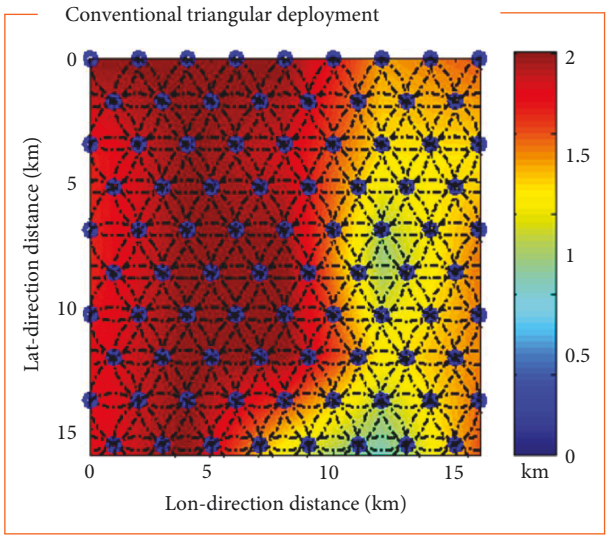

Figure 17: Deployment result using conventional triangular deployment within a range of 2 km (case 2).

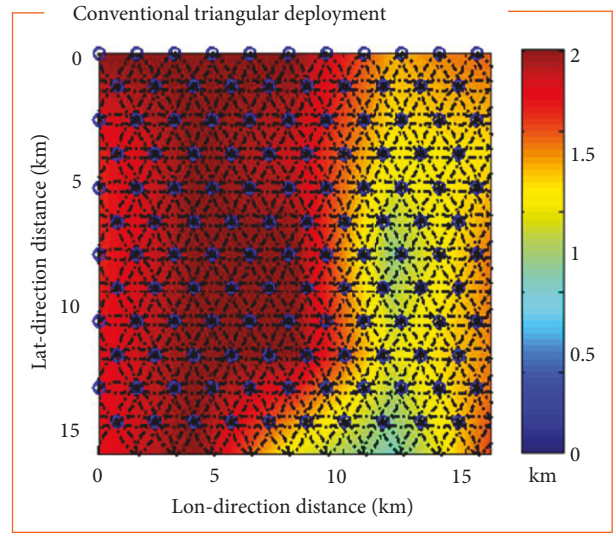

Figure 18: Deployment result using conventional triangular deployment within a range of 1.5 km (case 3).

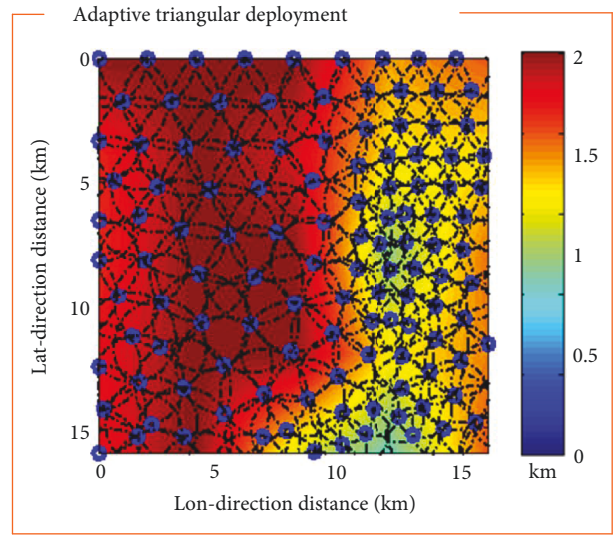

Figure 19: Deployment result using adaptive triangular deployment (case 4).

communication performance are not connected. In case 4, the connectivity to the entire area is achieved with a relatively small number of nodes.

The connectivity rates and number of nodes used to fill the given area for the four deployment cases are compared in Table 3. Here, the connectivity rate (R_c) is the ratio of the total number of nodes (N_t) deployed and the number of nodes (N_c) having k-connectivity ($k \geq 2$) and can be defined by Equation (5).

$$R_c = \frac{N_c}{N_t}. \quad (5)$$

In the case of a conventional triangular deployment assuming a communication range of 1 km (case 1), a total of 314 nodes are deployed in the given area, and each node has a connectivity rate of 100% as the communication range is satisfied for the entire target area. In this case, it is possible to implement a stable sensor network in a given area. However, it is an inefficient deployment as more nodes than necessary are deployed in an area having excellent communication performance. Assuming range of 2 km (case 2), the required number of nodes is 85, and the connectivity rate is approximately 30%. Assuming coverage of 1.5 km (case 3), the required number of nodes is 126 and the connectivity rate is about 70%. Cases 2 and 3 have a problem which the connectivity between the nodes is degraded since the number of nodes is insufficient in the area where the communication performance deteriorates. Therefore, the three cases do not satisfy the efficiency and stability of the network. When the

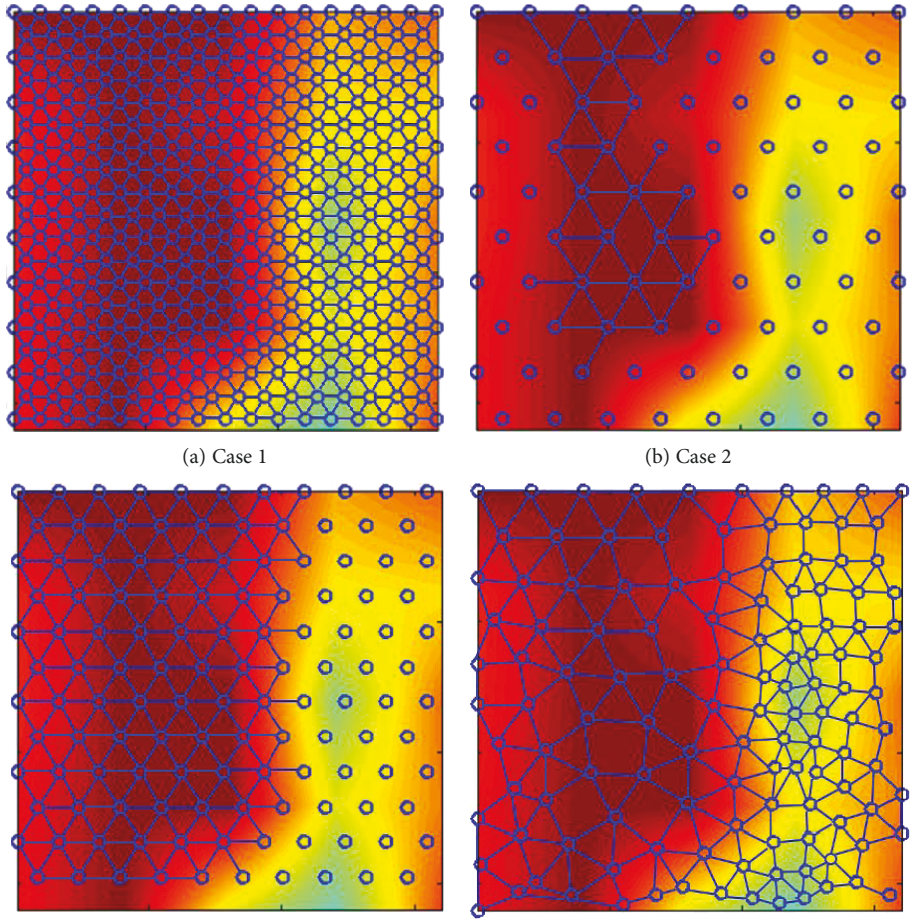

(a) Case 1 (b) Case 2

(c) Case 3 (d) Case 4

Figure 20: Connectivity of nodes for each case.

Table 3: Example of sensor deployment algorithm.

Case	Number of nodes	Number of connected node	Connectivity rate
1	314	314	100%
2	85	25	30%
3	126	88	70%
4	124	124	100%

adaptive triangular deployment algorithm (case 4) is used, 124 nodes are required. In this case, although the number of nodes is almost the same as that of case 3, the connectivity rate is 100% because each node is deployed through the interval adjustment considering the communication performance. Consequently, it can be observed that the adaptive triangular deployment is an algorithm that can achieve maximum connectivity with an optimal number of nodes.

5. Conclusion

In this paper, we propose an adaptive triangular deployment algorithm that can optimize connectivity in a sensor network as adjusting the spacing between nodes considering communication performance according to underwater environment. To consider the communication performance according to the underwater environment, actual location data from a sea such as sound velocity structure, seabed topography, and seabed constitution are collected. Using the collected data, the communication channel of the target area was simulated. A performance surface model was implemented by simulating the communication performance of the nodes according to their positions in the target area via the simulated communication channel. The conventional deployment algorithms mostly considered only the range of the nodes or connectivity under limited conditions. Further, most deployment algorithms have equally spaced nodes without considering the performance of the nodes according to the environment. The proposed adaptive triangular deployment algorithm can apply the performance surface model to adjust sensor intervals considering the communication ranges of the nodes according to their positions. Through this method, each node is guaranteed connectivity with its adjacent nodes and can achieve full connectivity. The proposed adaptive triangular deployment algorithm is thus demonstrated to be a suitable methodology for efficient and stable underwater

sensor network implementation that can secure maximum connectivity with an optimal number of nodes compared to the conventional triangular deployment algorithms.

Data Availability

The data used to support the findings of this study are included within the article.

Conflicts of Interest

The authors declare that there is no conflict of interest regarding the publication of this paper.

Acknowledgments

This work was supported by the Agency for Defense Development, Korea.

References

[1] M. Noori and M. Ardakani, "Efficient multiway relaying for data sharing in energy harvesting sensor networks," *Journal of Sensors*, vol. 2015, Article ID 285056, 8 pages, 2015.

[2] H. Zhang and J. C. Hou, "Is deterministic deployment worse that random deployment for wireless sensor networks?," in *Proceedings of the IEEE International Conference of Computer Communications (INFOCOM 2006)*, pp. 1–13, Barcelona, Spain, May 2006.

[3] L. Hong, "Deployment algorithm based on dynamic multi-populations particle swarm optimization for wireless sensor networks," *Computer Modelling & New Technologies*, vol. 18, no. 11, pp. 657–662, 2014.

[4] A. Dirafzoon, S. M. A. Salehizadeh, S. Emrani, and M. B. Menhaj, "Virtual force based individual particle optimization for coverage in wireless sensor networks," in *Electrical and Computer Engineering (CCECE 2010)*, pp. 1–4, Calgary, Canada, May 2010.

[5] F. Xiao, Y. Yang, R. Wang, and L. Sun, "A novel deployment scheme based on three-dimensional coverage model for wireless sensor networks," *The Scientific World Journal*, vol. 2014, Article ID 846784, 7 pages, 2014.

[6] L. C. Shiu, C. Y. Lee, and C. S. Yang, "The divide-and-conquer deployment algorithm based on triangles for wireless sensor networks," *IEEE Sensors Journal*, vol. 11, no. 3, pp. 781–790, 2011.

[7] B. Wang, H. Xu, W. Liu, and L. T. Yang, "The optimal node placement for Long Belt coverage in wireless networks," *IEEE Transactions on Computers*, vol. 64, no. 2, pp. 587–592, 2015.

[8] V. Isler, S. Kannan, and K. Daniilidis, "Sampling based sensor-network depoyment," in *International Conference on Intelligent Robots and Systems (iROS 2004)*, pp. 1780–1785, Sendai, Japan, September 2004.

[9] Y. C. Wang, C. C. Hu, and Y. C. Tseng, "Efficient deployment algorithms for ensuring coverage and connectivity of wireless sensor networks," in *Proceedings of the First International Conference Wireless Internet (WICON'05)*, Budapest, Hungary, July 2005.

[10] P. McDowell, *Environmental and Statistical Performance Mapping Model for Underwater Acoustic Detection Systems, [Ph.D. thesis]*, Department of Engineering and Applied Science, New Orleans University, New Orleans, LA, USA, 2010.

[11] Y. Fan and Z. Zilic, "BER testing of communication interfaces," *IEEE Transactions on Instrumentation and Measurement*, vol. 57, no. 5, pp. 897–906, 2008.

[12] M. B. Porter, *The BELLHOP Manual and User's Guide: Preliminary Draft*, Heat, Light and Sound Research, Inc., La Jolla, CA, USA, 2011.

[13] M. Felamban, B. Shihada, and K. Jamshaid, "Optimal node placement in underwater wireless sensor networks," in *2013 IEEE 27th International Conference on Advanced Information Networking and Applications (AINA)*, pp. 492–499, Barcelona, Spain, June 2013.

[14] G. M. Wenz, "Acoustic ambient noise in the ocean: spectra and sources," *The Journal of The Acoustical Society of America*, vol. 34, no. 12, pp. 1936–1956, 1962.

[15] F. D. Rango, F. Veltri, and P. Fazio, "A multipath fading channel model for underwater shallow acoustic communications," in *IEEE International Conference on Communications (ICC)*, pp. 3811–3815, Ottawa, ON, Canada, November 2012.

[16] M. R. Carnes, *Description and Evaluation of GDEM-V 3.0*, Memorandum Report Naval Research Laboratory, Hancock Country, MS, USA, 2009.

[17] C. Amante and B. W. Eakins, *ETOPO1 1 Arc-Minute Global Relief Model: Procedures, Data Sources and Analysis*, Memorandum Report National Geophysical Data Center, Boulder, CO, USA, 2009.